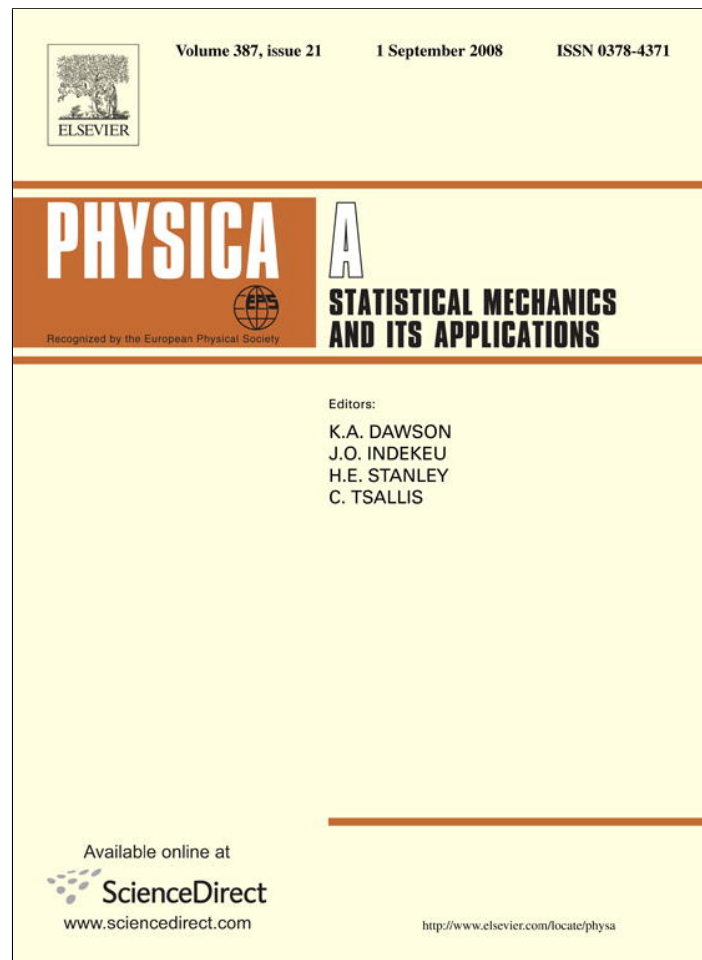


Provided for non-commercial research and education use.
Not for reproduction, distribution or commercial use.



This article appeared in a journal published by Elsevier. The attached copy is furnished to the author for internal non-commercial research and education use, including for instruction at the authors institution and sharing with colleagues.

Other uses, including reproduction and distribution, or selling or licensing copies, or posting to personal, institutional or third party websites are prohibited.

In most cases authors are permitted to post their version of the article (e.g. in Word or Tex form) to their personal website or institutional repository. Authors requiring further information regarding Elsevier's archiving and manuscript policies are encouraged to visit:

<http://www.elsevier.com/copyright>



Contents lists available at ScienceDirect

Physica A

journal homepage: www.elsevier.com/locate/physa

Local analysis of frustration based on Kagomé lattices

W. Lebrecht, J.F. Valdés, E.E. Vogel*

Departamento de Física, Universidad de La Frontera, Casilla 54-D, Temuco, Chile

ARTICLE INFO

Article history:

Received 26 February 2008
Received in revised form 1 May 2008
Available online 9 May 2008

PACS:
05.50.+q
75.10.Hk

Keywords:
Frustration
Kagomé lattices
Ising model

ABSTRACT

Magnetic frustration in the framework of the Edwards–Anderson model is studied for the ground level ($T = 0$) of the Kagomé lattice (KL). A sample consists of a realization of a random distribution of ferromagnetic (F) and antiferromagnetic (AF) interactions of the same strength along lines connecting nearest neighbors. Our goal is to compare two methods to calculate the following parameters: ground state energy, frustration and average frustration segment as functions of x , the concentration of F bonds. In doing so we make use of topological concepts such as plaquettes and frustration segments. The probability of a plaquette being unfrustrated (or flat) is $\wp_p(x)$, while the probability of a plaquette being frustrated (or curved) is $\wp_c(x)$. The analysis is done locally on a representative portion of the lattice which is called cell; cells of two different sizes are used in the present work. One method (which is simpler) is based on the probability function of any plaquette configuration $\phi(\wp_p, \wp_c)$. The other method is more exact but also more complex and increasingly difficult to use for large cells; it is based on the probability of bond configurations $\psi(x)$. These methods are compared between themselves noting that the simpler method can be enough for most of the range for x . In addition, numerical simulations for many random samples at different concentrations x for a size given by 75 spins with periodic boundary conditions were done. This provides reference lines to compare with the properties under study. The local frustration analysis to obtain both $\phi(\wp_p, \wp_c)$ and $\psi(x)$ is done over two cells of different size. Robustness of the criteria used in the local frustration analysis is also investigated.

© 2008 Elsevier B.V. All rights reserved.

1. Introduction

A frustrated system is based on the competition of interactions [1] that generate disorder within the system, and therefore its entropy is characterized by positive real numbers [2] even at zero temperature. This behavior is observed in spin-glasses [3], and in other geometrically frustrated magnetic materials [4,5].

To describe such systems Edwards and Anderson introduced decades ago a model [6] which has proved to be useful not only for spin glasses but for other complex systems. From our perspective we can describe this model as a regular lattice (two or three dimensions) where an Ising spin S occupy sites i over the lattice and exchange interactions J_{ij} lay along nearest-neighbor bonds. This J_{ij} is negative ($-J$, assuming a positive value for J) for ferromagnetic (F) interactions and positive (J) for antiferromagnetic (A) interactions in the so-called bimodal distribution. Then the Ising Hamiltonian of the system is given by:

$$H = \frac{1}{2} \sum_{i \neq j} J_{ij} S_i S_j. \quad (1)$$

* Corresponding author. Tel.: +56 45 325316; fax: +56 45 325323.
E-mail address: ee_vogel@ufro.cl (E.E. Vogel).

Let us designate by x the relative concentration of F bonds, so $(1 - x)$ corresponds to the concentration of A bonds. Such a mixture of bonds is randomly distributed through the sample. The resulting system is very complex, not all interactions can be simultaneously satisfied due to frustration and the configuration space can be thought as a multivalley energy landscape.

Most of the studies are done for square lattices (2D) and cubic lattices (3D). However, results are different according to geometry. Thus, for instance the ground state energy per bond is -0.70 for square lattices, -0.56 for triangular lattices and -0.82 for hexagonal lattices. Other 2D Archimedean lattices are less studied although their results are quite interesting since frustration happens in different ways as geometrical and topological conditions are changed. A Table comparing properties of the Edwards–Anderson model for different (not all) Archimedean lattices has been given elsewhere [7]. In present study we concentrate on the Kagomé lattice (KL) due to the nice feature of combining triangular and hexagonal geometries as discussed below.

Moreover, the emphasis here is on analytic methods since most of the reported results are obtained numerically. Although it is impossible to provide a full analytic treatment for such complex disordered system, the interpretation of the numerical results can benefit from theoretical approaches providing approximate functions reflecting the main tendencies for each particular lattice. To obtain analytic functions we will follow two independent methods which produce almost equivalent results. In addition and for comparison purposes we also perform numeric simulations for Kagomé lattices of size $N = 75$ spins, where periodic boundary conditions are assumed. Numeric simulations require several random distributions of F and AF bonds each one called a sample.

Let us now briefly review some useful concepts, while we focus on the parameters to be reported below. The minimum closed circuit in the lattice (triangle or hexagon for KL) is called plaquette. Plaquettes with odd number of AF bonds are said to be curved or frustrated since it is not possible to satisfy all interaction requirements when going around the plaquette.

Let us consider one particular state, α say, characterized by an ordered collection of spin orientations over the N sites, namely, $\{\dots \uparrow\downarrow\uparrow\downarrow \dots\}$. If parallel spins ($\uparrow\uparrow$ or $\downarrow\downarrow$) sit at the ends of a A bond the contribution to the energy is $+J$; let B_1 be the number of such bonds for state α . When antiparallel spins ($\uparrow\downarrow$ or $\downarrow\uparrow$) sit at the end of a F bond of the lattice the contribution to the energy of state α is $+J$; let B_2 be the number of these spins for state α . Similarly B_3 is the number of F bonds surrounded by parallel spins and B_4 is the number of A bonds between antiparallel spins. Then, the energy of state α can be written as

$$E^\alpha = JB_1 + JB_2 - JB_3 - JB_4, \tag{2}$$

where $B = \sum_{i=1}^4 B_i$ is the total number of bonds, which can be expressed in terms of the coordination number c and size of the system as $B = \frac{cN}{2}$. We can express energy in units of J (equivalent to making $J = 1$ in previous equation) which allows a straightforward splitting in terms of negative and positive contributions to the total energy. Bonds contributing positively to the energy are frustrated and the total number of them is denoted by $\Lambda^\alpha(N, x)$, the *frustration length*. Then we can rewrite the expression for the energy of state α as:

$$E^\alpha(c, N, x) = -(B_3 + B_4) + (B_1 + B_2) = -\frac{1}{2}cN + 2\Lambda^\alpha(N, x). \tag{3}$$

Thus, the ground state energy is now found upon minimizing the frustration length until its minimum possible value $\Lambda_g(N, x)$ is found, leading to the ground state energy of the system. $\Lambda_g(N, x)$ can be thought of as the sum of *frustration segments* each one joining the center of pairs of frustrated plaquettes in an optimized way leading to a minimum $\Lambda_g(N, x)$ value [8]. Let us designate the number of frustrated plaquettes by $P_c(c, N, x)$ which is determined by the probability $\wp_c(x)$ [9] of getting a frustrated plaquette according to the bonds that define it:

$$P_c(c, N, x) = P(c, N)\wp_c(x) = \frac{(c-2)}{2}N\wp_c(x). \tag{4}$$

The number of frustration segments is half this number; this leads us to an expression for the average frustration segment for any ground state of the system:

$$\langle \lambda_g(x) \rangle = \frac{2\Lambda_g(N, x)}{P_c(c, N, x)}. \tag{5}$$

After appropriately combining previous equations we get an expression for the ground state energy of the system:

$$E_g(c, N, x) = -\frac{1}{2}cN + \langle \lambda_g(x) \rangle N\wp_c(x) \frac{(c-2)}{2}, \tag{6}$$

where all elements coming into this equations have been previously defined.

2. Model

Average frustration segment $\langle \lambda_g(x) \rangle$, ground state energy per interaction $\varepsilon_g(x) = E_g(c, N, x)/B$, and frustration, $f_g(x) = 1 - h_g(x)$ of the diluted lattice will be reported in terms of analytical expressions, using two different approaches. Here $h_g(x)$ corresponds to the fraction of unfrustrated interactions [10]. Frustration f_g is directly related to the diluted lattice which

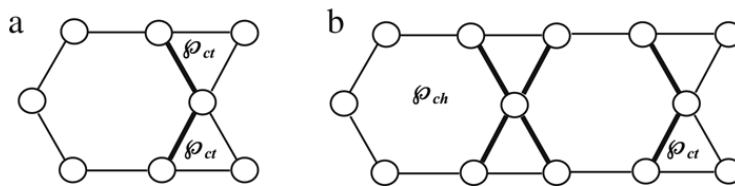


Fig. 1. (a) Representative cell 1 characterized by a maximum frustration segment of length 2; (b) Representative cell 2 whose maximum frustration segment has a length 3. $\wp_{ct}(x)$ ($\wp_{ch}(x)$) represents the probability that any triangular plaquette (hexagonal plaquette) is curved. Inner bonds represented by thicker lines are considered in the local frustration analysis for each cell.

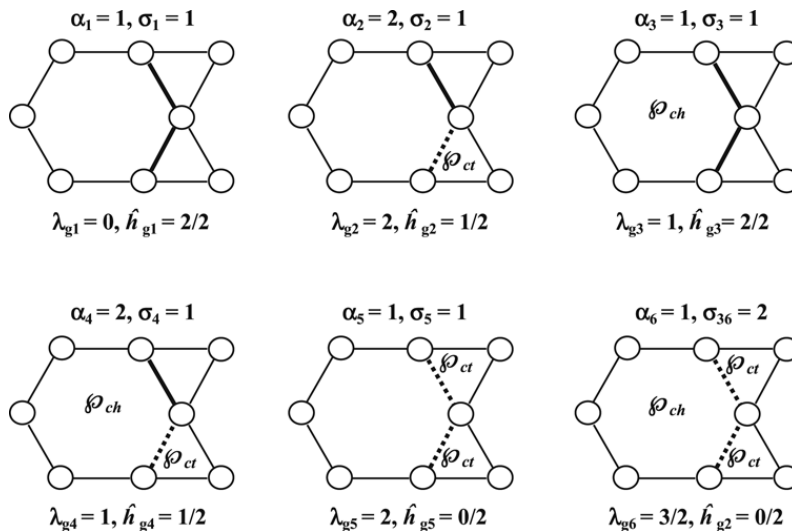


Fig. 2. The 6 families representing the combinatorics of flat and curved plaquettes over representative cell 1. Degeneracy α_j , number of frustration segments σ_j , average frustration length λ_{gj} , and fraction of unfrustrated bonds \hat{h}_{gj} are indicated for each family.

determines the ground manifold of the system [11]. Although we do not attempt a description based on the states of the system, it is worthwhile showing that both methods can be extended into that direction.

The starting point is the choice of a representative cell for KL over which a local analysis of frustration will be performed by means of topological analysis [12]. Two different representative cells associated to Kagomé lattice will be considered as illustrated in Fig. 1, where cell (b) is twice as large as cell (a); circles represent spin sites and lines illustrate exchange interactions of any kind.

The reason we have chosen KL for the present analysis flows from a closer examination of Fig. 1. Regardless of the size of the cell, there is always the mixture of plaquettes with odd number of bonds (triangular) which have an intrinsic frustration in the AF phase and plaquettes with an even number of bonds (hexagonal) which are free of frustration in the AF phase. Additionally both kind of plaquettes will face accidental frustration for any given x . So the functions describing the behavior of KL are non-trivial over the entire range $[0.0,1.0]$ for x . Thus, for instance, the nearby hexagonal lattice, consisting of only hexagonal plaquettes, will be described by functions that are symmetric with respect to $x = 0.5$. So, KL is a lattice with more possibilities for the analysis intended here to compare two different methods to deal with the local frustration.

Cell (a) is formed by three plaquettes and there are 6 possible generic plaquette configurations or families as illustrated in Fig. 2. Cell (b) has 36 possible families as illustrated in Figs. 4 and 5 later on. The larger the cell, the longer the maximum frustration segment that is allowed in the local frustration analysis. This is illustrated in Fig. 1 by means of the plaquette distribution showing the longest possible frustration segment in each case. In cell (a) the two curved plaquettes shown can be joined by a line going over the center of plaquettes going over 2 bonds, namely, the corresponding frustration segment has length 2. In cell (b) the segment joining the two most distant curved plaquettes has a length 3. The local analysis considers frustration over the internal bonds which are shown as thicker lines in Fig. 1: 2 for cell (a) and 6 for cell (b).

The number of families associated to representative cell 1 is 6 (while it is 36 for to representative cell 2). For each family we calculate the average frustration segment, energy per bond and frustration (relative number of internal frustrated bonds with respect to the total internal bonds of the cell). This is illustrated in Fig. 2 (Figs. 4 and 5) for cell 1 (cell 2).

The average frustration segment and the total frustration for any representative cell are given by:

$$\langle \lambda_g(x) \rangle = \frac{\sum_{j=1}^{\eta} \alpha_j \sigma_j \xi_j(x) \lambda_{gj}}{\sum_{j=1}^{\eta} \alpha_j \sigma_j \xi_j(x)}, \quad f_g(x) = 1 - h_g(x) = 1 - \sum_{j=1}^{\eta} \alpha_j \xi_j(x) \hat{h}_{gj}, \quad (7)$$

where the index j runs over the η families of the cell, α_j indicates the degeneracy of the j -th family, σ_j gives the corresponding number of local frustration segments, λ_{gj} is the length of the dominant local frustration segment and \hat{h}_{gj} is the relative size of the unfrustrated inner lattice (inner bonds); criteria for the local frustration analysis are given later on. The function $\xi_j(x)$ is generic here and represents the probability weight for that family and can be calculated by two different methods to be introduced shortly below.

The average energy per interaction associated to the ground level for any representative cell can be expressed as:

$$\langle \varepsilon_g(x) \rangle = -1 + \frac{\wp_c(x) \langle \lambda_g(x) \rangle}{c} (c - 2). \quad (8)$$

Independently of the way the representative cell is chosen we have at our disposal two different methods to calculate the probability $\xi_j(x)$ of each possible family:

(A) *Method based on plaquettes.* This is based on the probability for each distribution of flat and curved plaquettes, where the generic $\xi_j(x)$ function above is replaced by $\phi_j(\wp_p(x), \wp_c(x))$ to explicitly represent this method. The probabilities for triangular and hexagonal curved (and flat) plaquettes were already obtained [6]. Then $\phi_j(\wp_p(x), \wp_c(x))$ is simply given by a product where the number of factors is the number of plaquettes in the cell and the nature of each factor is decided by the form of the plaquette (hexagonal or triangular) and the corresponding topology (frustrated or flat) [13]. Thus for instance, for the second family in Fig. 2 we have: $\phi_2(\wp_p(x), \wp_c(x)) = \wp_{ph}(x) \wp_{pt}(x) \wp_{ct}(x)$.

(B) *Method based on bonds.* This is based on the probability for distributing all the possible configurations of ferromagnetic and antiferromagnetic bonds determining each family. This time the generic $\xi_j(x)$ is replaced $\psi_j(x)$. Such probability is found by the sum of all configurations of the bonds in the cell that built the family. Thus, for the second family we have: $\psi_2(x) = \sum_{i=0}^b c_{i2} x^{b-i} (1-x)^i$, where b is the number of bonds in the cell; The coefficients c_{ij} take into account the degeneracy of each bond distribution behind each distribution of F and AF bonds (these coefficients were already reported for cell 1 [12] and will be tabulated for cell 2 later on).

(C) *Numerical simulations.* To compare results obtained by the two methods presented above we did numerical simulations on samples of size $N = 75$ spins on a KL. The concentration of ferromagnetic bonds x was varied in the interval [0.0, 1.0] at steps of 0.05. The reported values correspond to average values over 500 randomly prepared samples for each concentration.

The main purpose of the present paper is to show that method 1, although simpler in its structure gives results similar to method 2 (which is exact but faces early size limitations). The numerical results draw a baseline for comparing the tendencies of both methods.

The local frustration analysis is based on the way curved plaquettes are connected in pairs by means of frustration segments. Such *plaquette connectivity* is done according to the following criteria: (a) If the number of curved plaquettes in the cell is even, they are connected inside cell, (b) If the number of curved plaquettes is odd, the remaining plaquette is connected externally minimizing energy, and (c) the fraction of satisfied interactions (bonds) is calculated considering only the internal bonds converging into a site. As an example, the second family for cell 1 contains one curved triangular plaquette, so criterium (b) is applied; the other curved plaquette is assumed immediately outside the perimeter with a maximum probability of being of length 2, crossing one internal bond, so its average frustration length is 2 (total frustration length/number of frustration segments = $2/1 = 2$). Applying criterium (c) one of two internal bonds is frustrated, so the fraction of unfrustrated bonds \hat{h}_g is $1/2$. This procedure is applied to all families shown in Fig. 2 (Figs. 4 and 5) for cell 1 (cell 2). For each family only curved plaquettes (\wp_{ct} and \wp_{ch}) are shown so all other plaquettes are flat. Internal frustrated bonds are represented by dotted lines.

3. Results and discussion

We present the results and discussions for each of the properties defined above, using both models for each of the two representative cells defined in Fig. 1. In Section 3.1 we do the analysis for cell 1; In Section 3.2 we proceed with cell 2; Finally, in Section 3.3 we introduce a correction to results on both cells for the case when there is an odd number of curved plaquettes in the cell.

3.1. Representative cell 1

Evaluation of Eq. (7) in terms of the polynomial function $\phi_j(\wp_p, \wp_c)$ and using parameters given in Fig. 2, method 1 for cell 1 yields:

$$\langle \lambda_{g11}(x) \rangle = \frac{4\wp_{ph}\wp_{pt}\wp_{ct} + \wp_{ch}\wp_{pt}^2 + 2\wp_{ch}\wp_{pt}\wp_{ct} + 2\wp_{ph}\wp_{ct}^2 + 3\wp_{ch}\wp_{ct}^2}{\wp_{ph}\wp_{pt}^2 + 2\wp_{ph}\wp_{pt}\wp_{ct} + \wp_{ch}\wp_{pt}^2 + 2\wp_{ch}\wp_{pt}\wp_{ct} + \wp_{ph}\wp_{ct}^2 + 2\wp_{ch}\wp_{ct}^2}, \quad (9)$$

$$f_{g11}(x) = 1 - (\wp_{ph}\wp_{pt}^2 + \wp_{ph}\wp_{pt}\wp_{ct} + \wp_{ch}\wp_{pt}^2 + \wp_{ch}\wp_{pt}\wp_{ct}), \quad (10)$$

where we have omitted the explicit dependence on x for simplicity; the condition $\wp_{ph}(x) + \wp_{ch}(x) = \wp_{pt}(x) + \wp_{ct}(x) = 1$ is satisfied for all x . We make use of the distribution functions for curved plaquettes, $\wp_c(x)$ for hexagonal and triangular plaquettes previously developed [9].

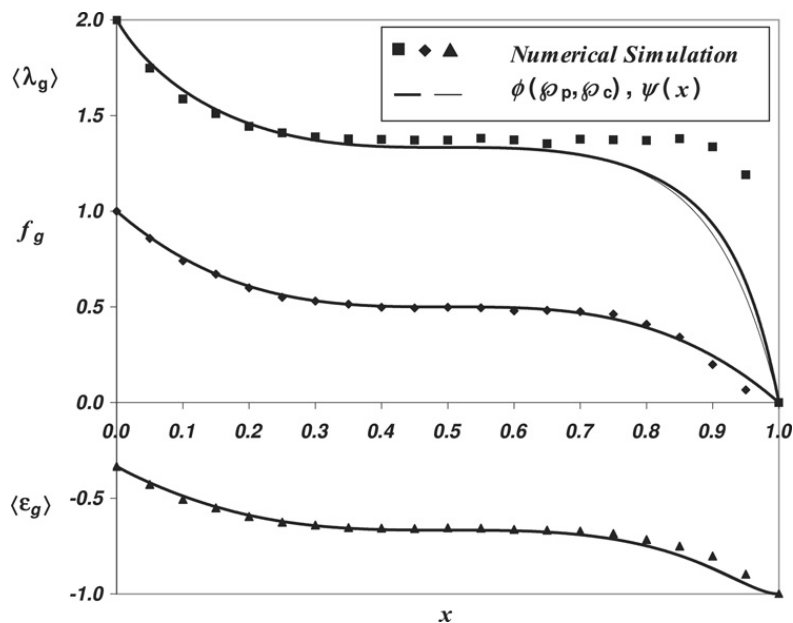


Fig. 3. Representative cell 1 is used. Functions obtained by means of method 1 and method 2 are plotted for average frustration segment, frustration of diluted lattice and average energy per interaction associated to the ground level, where the independent variable x is the concentration of F bonds. Moreover, symbols indicates configurational average values for the same magnitudes obtained through numerical simulations over 500 random samples (75 spins) for different ferromagnetic concentrations.

On the other hand, with the aid of polynomial function for bonds $\psi_j(x)$ used by method 2, we get for cell 1:

$$\langle \lambda_{g21}(x) \rangle = \frac{4\psi_2 + \psi_3 + 2\psi_4 + 2\psi_5 + 3\psi_6}{\psi_1 + 2\psi_2 + \psi_3 + 2\psi_4 + \psi_5 + 2\psi_6}, \quad (11)$$

$$f_{g21} = 1 - (\psi_1 + \psi_2 + \psi_3 + \psi_4). \quad (12)$$

Each one of the polynomial functions $\psi_j(x)$ associated to the representative cell 1 was already reported for this lattice [12]. Making use of such results we get:

$$\langle \lambda_{g21}(x) \rangle = \frac{2(1-x)(1+2x[1-10x+44x^2-96x^3+128x^4-96x^5+32x^6])}{1+4x(1-8x+31x^2-70x^3+98x^4-84x^5+40x^6-8x^7)}, \quad (13)$$

$$f_{g21} = 1 - x(3 - 6x + 4x^2). \quad (14)$$

Fig. 3 shows the behavior of functions given in Eqs. (8), (9), (10), (13) and (14) associated to cell 1.

Independently, a numerical calculation through multireplica method varying the concentration of x in the range $[0, 1]$ with increments $D(x) = 0.05$ was done for a lattice with 75 spins. Results represented by filled symbols represent average values over 500 randomly prepared samples for each concentration.

Results produced by the two methods are almost undistinguishable and some slight differences arise for $\lambda_g(x)$ near $x = 0.9$ only. However, a better coincidence is observed for the parameters with direct physical meaning: $f_g(x)$ and $\varepsilon_g(x)$. The comparison to the numerical results is also better for method 1. Numerical simulations tend to give a larger average frustration segment towards the ferromagnetic domain ($x \rightarrow 1.0$). This is eventually due to the possibility of existence of just a few curved plaquettes far away from each other. Although such configuration happens in a lattice with 75 spins or larger with a manifestation in the topological parameter $\langle \lambda_g(x) \rangle$, the statistical weight of this configuration is minimal when calculating frustration in the physical lattice or ground state energy.

3.2. Representative cell 2

The procedure is illustrated in Figs. 4 and 5 for each one of 36 families the set. Here, we have labeled only triangular- and hexagonal curved plaquettes, where the non-labeled ones must be assumed as flat plaquettes.

We begin by evaluating Eq. (7) by method 1, namely, upon evaluation of the polynomial function $\phi_j(\delta_p, \delta_c)$, with the parameters given in Figs. 4 and 5, through the auxiliary functions $\phi_N(\delta_p, \delta_c)$ and $\phi_D(\delta_p, \delta_c)$. Then we get:

$$\langle \lambda_{g12} \rangle = \frac{\phi_N(\delta_p, \delta_c)}{\phi_D(\delta_p, \delta_c)}, \quad (15)$$

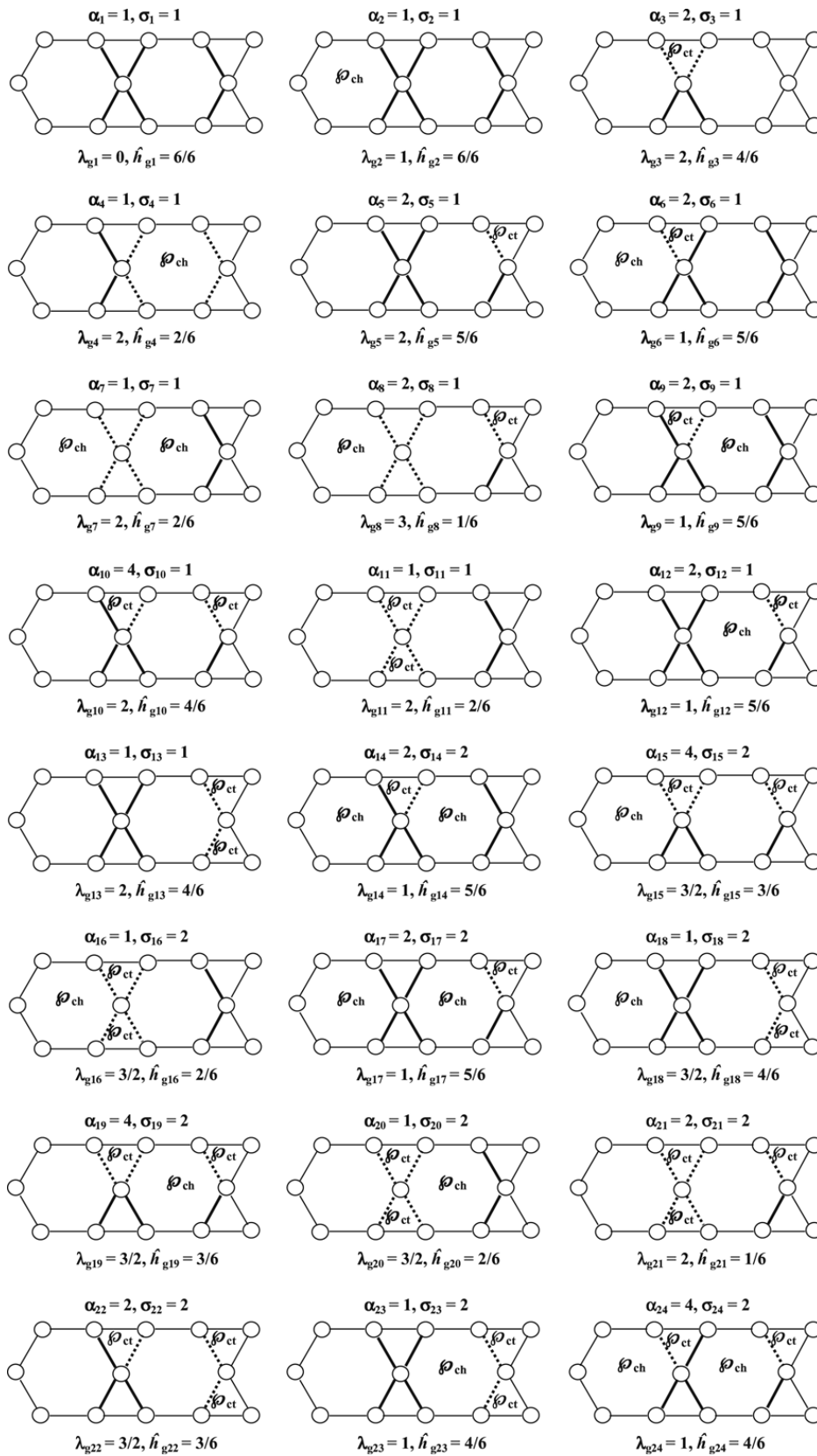


Fig. 4. The first 24 families (of a total of 36) representing the combinatorics of flat and curved plaquettes over representative cell 2. Symmetry α_j , number of frustration segments σ_j , average frustration length λ_{gj} , and fraction of unfrustrated bonds \hat{h}_{gj} are indicated for each family.

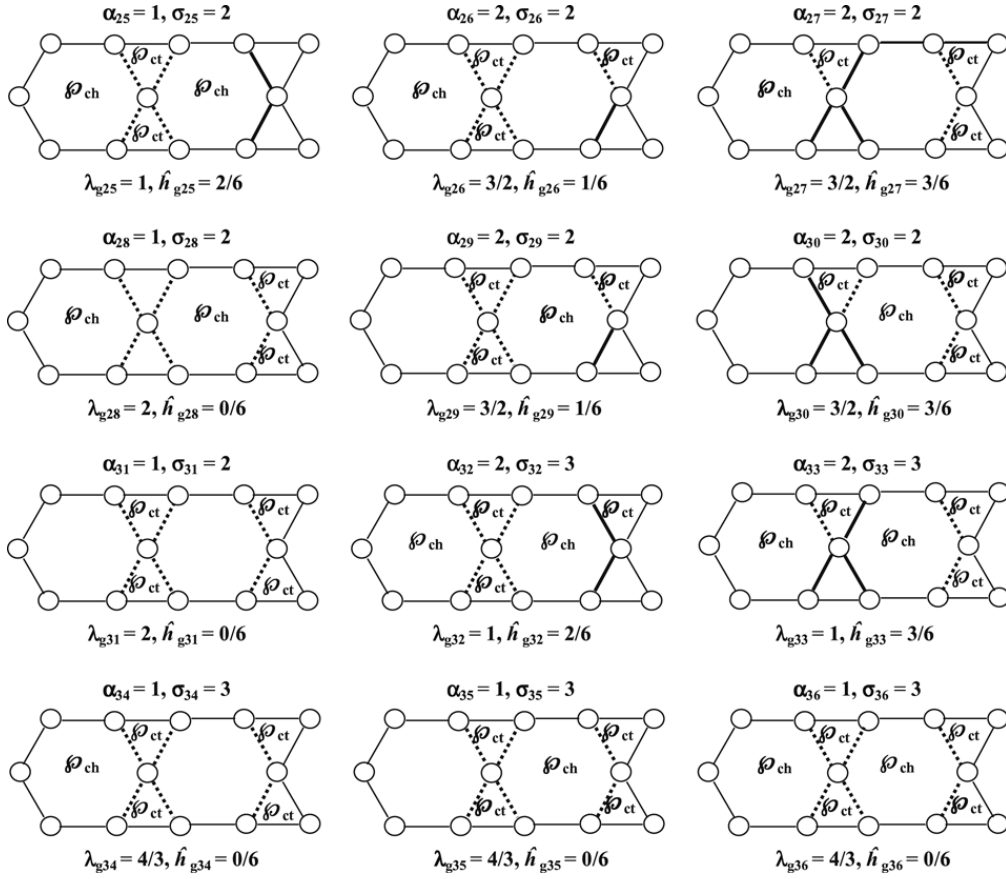


Fig. 5. The last 12 families representing the combinatorics of flat and curved plaquettes over representative cell 2. Symmetry α_j , number of frustration segments σ_j , average frustration length λ_{gj} , and fraction of unfrustrated bonds \hat{h}_{gj} are indicated for each family.

where:

$$\begin{aligned} \phi_N(\delta_p, \delta_c) &= 3\delta_{ch}\delta_{ph}\delta_{pt}^4 + 8\delta_{ph}^2\delta_{ct}\delta_{pt}^3 + 12\delta_{ch}\delta_{ph}\delta_{ct}\delta_{pt}^3 + 2\delta_{ch}^2\delta_{pt}^4 \\ &+ 12\delta_{ph}^2\delta_{ct}^2\delta_{pt}^2 + 8\delta_{ch}^2\delta_{ct}\delta_{pt}^3 + 35\delta_{ch}\delta_{ph}\delta_{ct}^2\delta_{pt}^2 + 14\delta_{ph}^2\delta_{ct}^3\delta_{pt} \\ &+ 14\delta_{ch}^2\delta_{ct}^2\delta_{pt}^2 + 24\delta_{ch}\delta_{ph}\delta_{ct}^3\delta_{pt} + 4\delta_{ph}^2\delta_{ct}^4 + 12\delta_{ch}^2\delta_{ct}^3\delta_{pt} + 8\delta_{ch}\delta_{ph}\delta_{ct}^4 + 4\delta_{ch}^2\delta_{ct}^4, \\ \phi_D(\delta_p, \delta_c) &= \delta_{ph}^2\delta_{pt}^4 + 2\delta_{ch}\delta_{ph}\delta_{pt}^4 + 4\delta_{ph}^2\delta_{ct}\delta_{pt}^3 + 8\delta_{ch}\delta_{ph}\delta_{ct}\delta_{pt}^3 \\ &+ \delta_{ch}^2\delta_{pt}^4 + 6\delta_{ph}^2\delta_{ct}^2\delta_{pt}^2 + 8\delta_{ch}^2\delta_{ct}\delta_{pt}^3 + 24\delta_{ch}\delta_{ph}\delta_{ct}^2\delta_{pt}^2 \\ &+ 8\delta_{ph}^2\delta_{ct}^3\delta_{pt} + 12\delta_{ch}^2\delta_{ct}^2\delta_{pt}^2 + 16\delta_{ch}\delta_{ph}\delta_{ct}^3\delta_{pt} + 2\delta_{ph}^2\delta_{ct}^4 + 12\delta_{ch}^2\delta_{ct}^3\delta_{pt} + 6\delta_{ch}\delta_{ph}\delta_{ct}^4 + 3\delta_{ch}^2\delta_{ct}^4. \end{aligned}$$

Frustration of the inner lattice, can be summarized in terms of the auxiliary functions $h_1(\delta_p, \delta_c)$ and $h_2(\delta_p, \delta_c)$ in the following way:

$$\langle f_{g12}(x) \rangle = 1 - \frac{1}{6}(h_1(\delta_p, \delta_c) + h_2(\delta_p, \delta_c)), \quad (16)$$

where:

$$\begin{aligned} h_1(\delta_p, \delta_c) &= 6\delta_{ph}^2\delta_{pt}^4 + 8\delta_{ch}\delta_{ph}\delta_{pt}^4 + 18\delta_{ph}^2\delta_{ct}\delta_{pt}^3 + 32\delta_{ch}\delta_{ph}\delta_{ct}\delta_{pt}^3 + 2\delta_{ch}^2\delta_{pt}^4 + 22\delta_{ph}^2\delta_{ct}^2\delta_{pt}^2, \\ h_2(\delta_p, \delta_c) &= 20\delta_{ch}^2\delta_{ct}\delta_{pt}^3 + 36\delta_{ch}\delta_{ph}\delta_{ct}^2\delta_{pt}^2 + 8\delta_{ph}^2\delta_{ct}^3\delta_{pt} + 18\delta_{ch}^2\delta_{ct}^2\delta_{pt}^2 + 16\delta_{ch}\delta_{ph}\delta_{ct}^3\delta_{pt} + 10\delta_{ch}^2\delta_{ct}^3\delta_{pt}. \end{aligned}$$

We apply now method 2 to cell 2. This can be expressed by means of the auxiliary functions $f_1(\psi_j)$ and $f_2(\psi_j)$, as:

$$\langle \lambda_{g22}(x) \rangle = \frac{f_1(\psi_j)}{f_2(\psi_j)}, \quad (17)$$

where:

$$\begin{aligned} f_1(\psi_j) &= \psi_2 + 4\psi_3 + 2\psi_4 + 4\psi_5 + 2\psi_6 + 2\psi_7 + 6\psi_8 + 2\psi_9 + 8\psi_{10} + 2\psi_{11} + 2\psi_{12} + 2\psi_{13} + 4\psi_{14} + 12\psi_{15} \\ &+ 3\psi_{16} + 4\psi_{17} + 3\psi_{18} + 12\psi_{19} + 3\psi_{20} + 8\psi_{21} + 6\psi_{22} + 2\psi_{23} + 8\psi_{24} + 2\psi_{25} + 6\psi_{26} + 6\psi_{27} \\ &+ 4\psi_{28} + 6\psi_{29} + 6\psi_{30} + 4\psi_{31} + 6\psi_{32} + 6\psi_{33} + 4\psi_{34} + 4\psi_{35} + 4\psi_{36}, \\ f_2(\psi_j) &= \psi_1 + \psi_2 + 2\psi_3 + \psi_4 + 2\psi_5 + 2\psi_6 + \psi_7 + 2\psi_8 + 2\psi_9 + 4\psi_{10} + \psi_{11} + 2\psi_{12} + \psi_{13} + 4\psi_{14} + 8\psi_{15} \\ &+ 2\psi_{16} + 4\psi_{17} + 2\psi_{18} + 8\psi_{19} + 2\psi_{20} + 4\psi_{21} + 4\psi_{22} + 2\psi_{23} + 8\psi_{24} + 2\psi_{25} + 4\psi_{26} \\ &+ 4\psi_{27} + 2\psi_{28} + 4\psi_{29} + 4\psi_{30} + 2\psi_{31} + 6\psi_{32} + 6\psi_{33} + 3\psi_{34} + 3\psi_{35} + 3\psi_{36}. \end{aligned}$$

Table 1

Probabilistic weight factors in term of $x^{18-i}(1-x)^i$ ($i = 0 - 18$) associated to distribution functions ψ_j ($j = 1 - 36$), given in Figs. 4 and 5

i	0	1	2	3	4	5	6	7	8	9	10	11	12	13	14	15	16	17	18
ψ_1	1	0	9	20	53	164	277	424	643	744	715	580	327	116	23	0	0	0	0
ψ_2	0	4	2	20	76	136	270	456	616	756	734	548	332	128	18	0	0	0	0
ψ_3	0	1	6	15	52	149	282	459	664	755	698	541	308	119	38	9	0	0	0
ψ_4	0	2	6	24	68	130	266	480	632	710	730	584	324	118	22	0	0	0	0
ψ_5	0	2	2	20	56	126	306	480	608	766	742	516	296	130	38	8	0	0	0
ψ_6	0	1	4	19	56	133	292	479	624	755	748	521	280	135	44	5	0	0	0
ψ_7	0	0	10	28	52	140	286	440	632	760	710	556	340	124	18	0	0	0	0
ψ_8	0	0	8	14	52	156	268	458	680	744	704	546	292	124	44	6	0	0	0
ψ_9	0	1	2	23	60	125	286	475	648	771	702	517	316	127	34	9	0	0	0
ψ_{10}	0	0	3	14	45	132	295	498	681	760	681	498	295	132	45	14	3	0	0
ψ_{11}	0	0	3	12	51	132	279	512	687	744	697	492	281	148	45	8	5	0	0
ψ_{12}	0	1	4	17	60	141	272	469	664	755	708	531	300	127	40	7	0	0	0
ψ_{13}	0	0	5	8	45	148	281	492	697	744	687	512	279	132	51	12	3	0	0
ψ_{14}	0	0	6	16	60	148	258	468	680	744	714	536	284	132	46	4	0	0	0
ψ_{15}	0	0	2	14	50	132	286	498	686	760	686	498	286	132	50	14	2	0	0
ψ_{16}	0	0	2	16	44	132	302	484	680	776	670	504	300	116	50	20	0	0	0
ψ_{17}	0	0	4	22	60	132	272	474	664	760	708	522	300	132	40	6	0	0	0
ψ_{18}	0	0	0	20	50	116	300	504	670	776	680	484	302	132	44	16	2	0	0
ψ_{19}	0	0	3	10	53	140	271	502	697	744	697	502	271	140	53	10	3	0	0
ψ_{20}	0	0	2	14	48	136	294	478	676	800	686	458	296	152	42	10	4	0	0
ψ_{21}	0	0	0	8	38	130	296	516	742	766	608	480	306	126	56	20	2	2	0
ψ_{22}	0	0	0	97	38	119	308	541	698	755	664	459	282	149	52	15	6	1	0
ψ_{23}	0	0	4	10	42	152	296	458	686	800	676	478	294	136	48	14	2	0	0
ψ_{24}	0	0	1	16	47	136	301	464	675	816	675	464	301	136	47	16	1	0	0
ψ_{25}	0	0	2	12	52	140	278	488	696	760	686	508	276	124	58	16	0	0	0
ψ_{26}	0	0	0	6	44	124	292	546	704	744	680	458	268	156	52	14	8	0	0
ψ_{27}	0	0	0	5	44	135	280	521	748	755	624	479	292	133	56	19	4	1	0
ψ_{28}	0	0	0	16	58	124	276	508	686	760	696	488	278	140	52	12	2	0	0
ψ_{29}	0	0	0	7	40	127	300	531	708	755	664	469	272	141	60	17	4	1	0
ψ_{30}	0	0	0	9	34	127	316	517	702	771	648	475	286	125	60	23	2	1	0
ψ_{31}	0	0	0	0	23	116	327	580	715	744	643	424	277	164	53	20	9	0	1
ψ_{32}	0	0	0	6	40	132	300	522	708	760	664	474	272	132	60	22	4	0	0
ψ_{33}	0	0	0	4	46	132	284	536	714	744	680	468	258	148	60	16	6	0	0
ψ_{34}	0	0	0	0	18	128	332	548	734	756	616	456	270	136	76	20	2	4	0
ψ_{35}	0	0	0	0	22	118	324	584	730	710	632	480	266	130	68	24	6	2	0
ψ_{36}	0	0	0	0	18	124	340	556	710	760	632	440	286	140	52	28	10	0	0

Similarly, frustration associated to diluted lattice is given by:

$$f_{g22} = 1 - \frac{1}{6}(g_1(\psi_j) + g_2(\psi_j)), \tag{18}$$

where the auxiliary functions $g_1(\psi_j)$ and $g_2(\psi_j)$ are expressed as:

$$g_1(\psi_j) = 6\psi_1 + 6\psi_2 + 8\psi_3 + 2\psi_4 + 10\psi_5 + 10\psi_6 + 2\psi_7 + 2\psi_8 + 10\psi_9 + 16\psi_{10} + 2\psi_{11} + 10\psi_{12} + 4\psi_{13} + 10\psi_{14} + 12\psi_{15} + 2\psi_{16} + 10\psi_{17},$$

$$g_2(\psi_j) = 4\psi_{18} + 12\psi_{19} + 2\psi_{20} + 2\psi_{21} + 6\psi_{22} + 4\psi_{23} + 16\psi_{24} + 2\psi_{25} + 2\psi_{26} + 6\psi_{27} + 2\psi_{29} + 6\psi_{30} + 4\psi_{32} + 6\psi_{33}.$$

Coefficients of polynomial functions $\psi_j(x)$ were obtained through a numerical procedure on representative cell 2 and they are shown in Table 1. These coefficients take into account different ways of distributing bonds for the j th family. First row of the table indicates the number of ferromagnetic bonds for the cell, this number varies between 0 and 18. On the other hand, each row represents the polynomial associated to each family of the set. Polynomial functions $\psi_j(x)$ can be constructed as:

$$\psi_j(x) = \sum_{i=0}^{18} c_{ij}x^{18-i}(1-x)^i, \tag{19}$$

where the sum of coefficients associated to each family satisfies the closure rule:

$$\sum_{i=0}^{18} c_{ij} = 2^{18-6} = 2^{12} = 4096, \tag{20}$$

where 18 is the total number of bonds in cell 2 while 6 is the total number of plaquettes in such cell.

A similar condition is also valid for representative cell 1, where the summation is extended from 0 to 10 (total number of bonds on cell 1) and considering as 3 the total number of plaquettes associated to such cell. Then, the sum of coefficients for this case is given by $2^{10-3} = 128$.

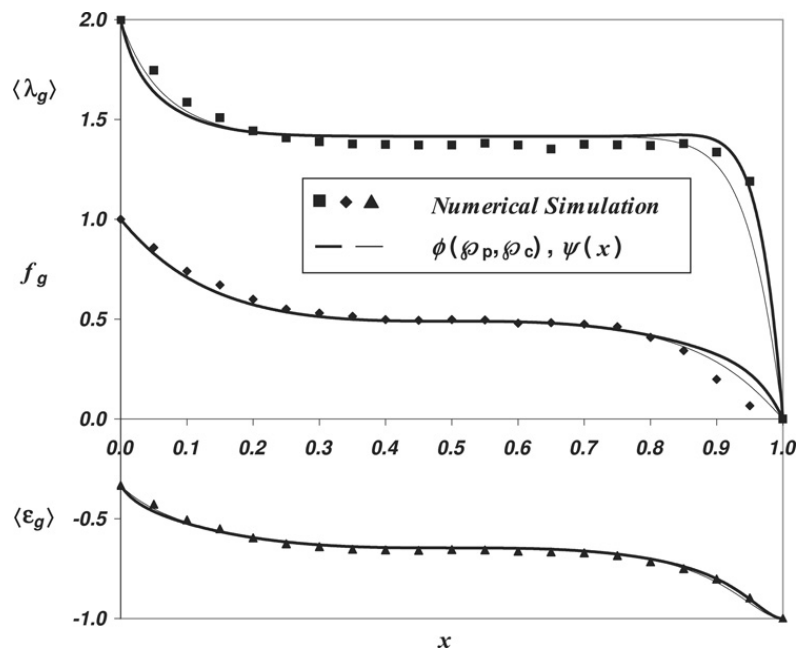


Fig. 6. Representative cell 2 is used. Functions obtained by means of method 1 and method 2 are plotted for average frustration segment, frustration of diluted lattice and average energy per interaction associated to the ground level, where the independent variable x is the concentration of F bonds. Same values obtained by numerical simulations are included here as a reference.

Average frustration length and total frustration of the diluted lattice as function of ferromagnetic concentration, x , are given by:

$$\langle \lambda_{g22}(x) \rangle = \frac{f_1(x)}{f_2(x)}, \tag{21}$$

where:

$$f_1(x) = 4 - 8x - 10x^2 + 268x^3 - 1538x^4 + 5386x^5 - 12654x^6 + 19544x^7 - 16720x^8 - 1312x^9 + 24320x^{10} - 33408x^{11} + 23808x^{12} - 9216x^{13} + 1536x^{14},$$

$$f_2(x) = 2 + 6x - 84x^2 + 512x^3 - 2077x^4 + 6226x^5 - 13904x^6 + 22676x^7 - 25916x^8 + 18608x^9 - 4832x^{10} - 5056x^{11} + 6144x^{12} - 2816x^{13} + 512x^{14},$$

and

$$f_{g22}(x) = 1 - \frac{g(x)}{6}, \tag{22}$$

where:

$$g(x) = 24x - 86x^2 + 258x^3 - 1118x^4 + 5516x^5 - 21748x^6 + 63240x^7 - 135584x^8 + 215008x^9 - 249792x^{10} + 206976x^{11} - 115968x^{12} + 39424x^{13} - 6144x^{14},$$

respectively.

Analytical results associated to the average frustration segment, frustration of diluted lattice, and energy per interaction associated to ground level for representative cell 2 are shown in Fig. 6. They correspond to evaluation of Eqs. (8), (15), (16), (21) and (22). The results of the numerical simulation for a lattice with 75 spins are also included in Fig. 6 for comparison.

Differences between the two methods remain very small for the larger lattice. This speaks clearly in favor of method 1 which is simpler to use since it makes use of previous expressions for curved and flat plaquettes without going into the details of the bond distribution. The agreement for the three parameters in the intermediate region ($0.2 < x < 0.8$, say) is remarkable. Both methods overestimate frustration towards the ferromagnetic phase. This could be due to the additional statistical weight that the frustration segments of length 3 get in the asymmetrical cell used here. Nothing of this seems to have a noticeable effect in the ground state energy where the agreement between the two methods and the comparison to the numerical results is excellent.

3.3. Refinement to plaquette connectivity

In previous analysis only the dominant frustration segment was considered for the connectivity in families with odd number of curves plaquettes according to previous criteria. Eventually, the connection to an odd plaquette can take along

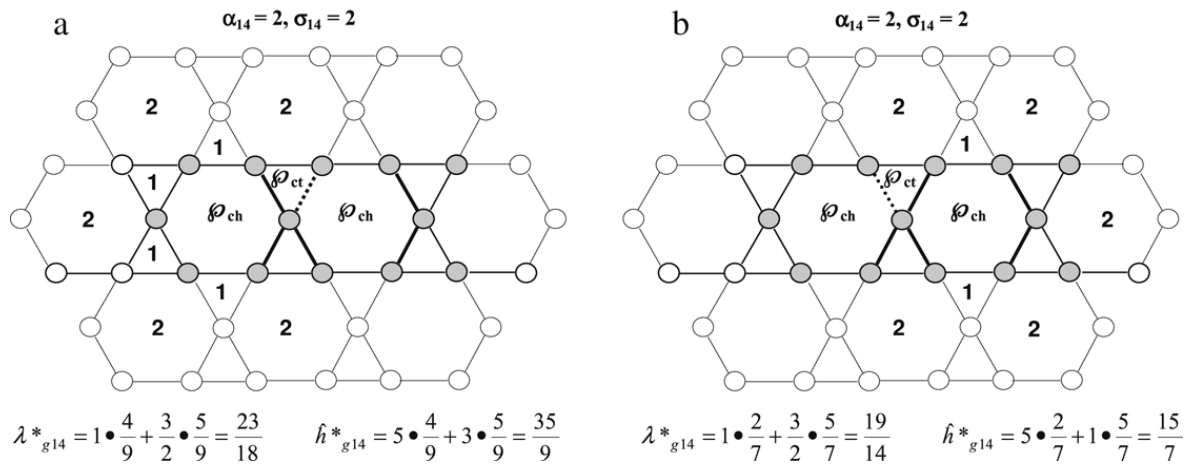


Fig. 7. The two possibilities of connecting frustrated plaquettes (a) and (b) associated to 14th-family of the set belonging to representative cell 2. The first case (a) represents the configuration of minimum energy.

with frustration segments of different lengths, each one with its corresponding statistical weight. This is precisely the idea in this subsection, where we choose cell 2 for the analysis.

As the idea is to discuss the importance (or not) of such a fractional frustration segment we will do the analysis reinforcing this purpose in a way that also seeks simplicity. That is, we will assign equal probability of connection to external plaquettes independently of the energy cost. Namely, all surrounding plaquettes have the same probability of being curved regardless of the geometry.

We will illustrate this idea by means of one example which can be used as a model for the rest of the analysis. Let us assume the odd plaquette in the analysis is the left hexagonal plaquette of cell 2 in the 14th family given in Fig. 4. If we match the only curved triangular plaquette to the curved hexagonal plaquette to the right with a segment of length 1, namely $\lambda_g = 1$, the odd plaquette is the curved hexagonal to the left as represented in Fig. 7(a). There are 4 external plaquettes that can connect to the odd plaquette with segments of length 1 ($\lambda_{ga} = 1$) and 5 external plaquettes that can connect to the odd plaquette with a segment of length 2 ($\lambda_{gb} = 2$). Within the equal probability approach outlined above we can write: $\lambda_{g14}^* = 1 \cdot \frac{4}{9} + \frac{3}{2} \cdot \frac{5}{9} = \frac{23}{18}$ and $\hat{h}_{g14}^* = 5 \cdot \frac{4}{9} + 3 \cdot \frac{5}{9} = \frac{35}{9}$.

However, this is not the only way to do the internal matching. In Fig. 7(b) we represent the situation in which the odd plaquette is the curved hexagonal plaquette to the right, in which case there are 2 possible external plaquettes connecting with segments of length 1, and 5 possible external plaquettes with segments of length 2. This leads to $\lambda_{g14}^* = \frac{19}{14}$ and $\hat{h}_{g14}^* = \frac{15}{7}$.

The configuration of minimum energy is given by Fig. 7(a) which corresponds to the one with the least value for λ_{g14}^* according to Eq. (3). Actually we have chosen family 14 in cell 2 because of this double possibility. This fact is also found in other families of cell 2 and it was always solved by choosing the connection with less energy involved.

Applying the analysis described above to all cases including an odd number of curved plaquettes for each family we recalculate the average frustration segment, frustration of diluted lattice and average energy per interaction for cell 2. The resulting functions are marked with an asterisk and they are illustrated in Fig. 8.

Not surprisingly $\langle \lambda_g^* \rangle$ is now larger for all x values when compared to previous results for cell 2 in Fig. 6. This is due to the equal probability assigned to frustration segments of length 1 and 2 as discussed above. However, the important fact here is that this is the same for both methods. This is also reflected to a less extent for the energy ε_g^* and it is hard to notice for \hat{h}_g^* . So, the analysis based on the dominant frustration segment seems to be good enough for the purposes of general tendencies in the determinations of properties as functions of x .

4. Conclusions

We have used two methods to calculate parameters associated to the frustration of Edwards–Anderson model on a Kagomé lattice. The simpler model (model 1) based on general functions for probability of frustration for curved plaquettes gives results that are almost undistinguishable from those calculated with a more complete model (model 2) based on the probability of frustration of every bond. As the study has considered the whole range of concentrations for F bonds, namely $0.0 \leq x \leq 1.0$, this conclusion is very general and important. Actually, the only noticeable differences appear towards the thermodynamic limit, for about $0.85 < x < 0.95$, where a large dispersion of configurations giving importance to long frustration segments is to be expected.

We have tested the stability of this conclusion along two lines of thought. First, upon increasing the size of the representative cell. Second, upon considering variations of the criteria for matching curved plaquettes when there is an odd number of them. We present next the conclusions of these two studies.

We duplicated the representative cell as shown in Fig. 1. Both methods show similar behavior as compared to the results obtained by the numerical simulation on a Kagomé lattice with 75 spins: the average frustration segment is overestimated

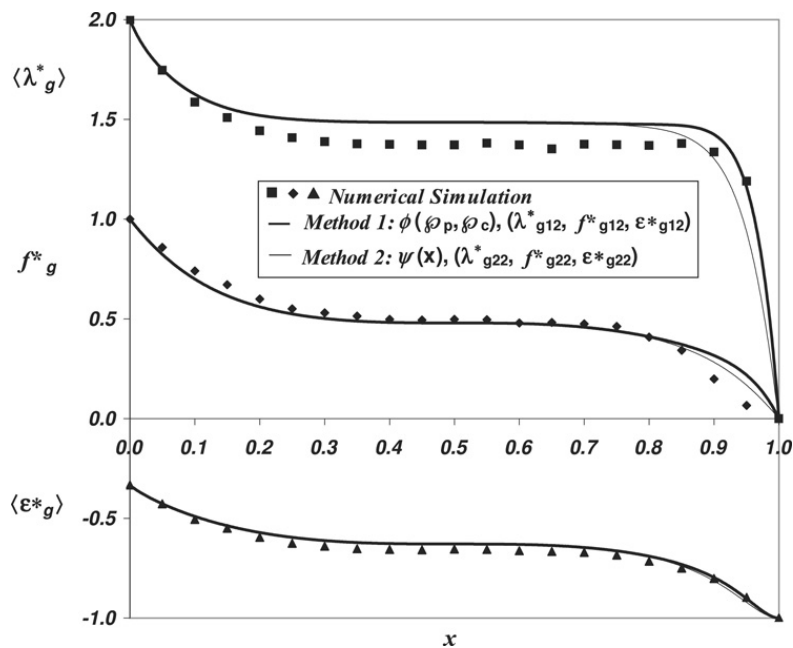


Fig. 8. Representative cell 2 is used. Functions obtained by means refined method 2 are plotted for average frustration segment, frustration of diluted lattice and average energy per interaction associated to the ground level, where the independent variable x is the concentration of F bonds. Same values obtained by numerical simulations are included here as a reference.

almost over the whole range, frustration is overestimated towards the ferromagnetic limit and average energy per bond looks well within the entire range. The former two observations are probably due to the fact that we have duplicated the representative cell, which turns out in an asymmetric enlargement of the cell thus favoring long segments along the preferred direction against the abundance of shorter segments in the transverse direction. This could eventually be solved by quadruplication of the initial cell (cell 1) but the analysis (especially using method 2) would be impossible within the framework of the present paper and it would not add much to the main purpose of this work which is to compare both methods to validate the simpler one.

On the other hand, we modified one of the criteria to match curved plaquettes to test the similarity of both methods. When there is an even number of plaquettes they are matched internally within the cell at the lowest possible energy. The doubt arises when there is an odd number of curved plaquettes and one of them (the odd plaquette) has to be matched outside with any possible length. We made use of the larger cell to test two criteria: (a) the most abundant or dominant frustration segment (usually of length 1) was the only one considered; (b) a mixture of segments of length 1 and 2, with equal probability, and weights given by the abundance of the matching plaquette. Two conclusions are obtained. First, this criterion favors larger average frustration segments. Second, and more relevant to the purposes of the present work, the effect of this criterion is the same for both methods which makes more robust the use of the simpler method 1 for further calculations.

All of the above indicates that method 1 is sufficiently good (and probably enough) to calculate physical and topological properties of frustrated systems like the Kagomé lattice with the Edwards–Anderson model for the case of variable concentration of F bonds. Since more accurate results are obtained as the representative lattice is enlarged (comprising and increasing number of plaquettes) method 2, based on each bond, faces difficulties when exhausting all possible combinations. Since the number of plaquettes is less than the number of bonds, the combination of plaquettes is easier to handle in the way introduced above as method 1. Moreover, this method is easier to implement in the computer by an appropriate algorithm even varying the geometry of the lattice. This is precisely what we have in mind for the continuation of this work after establishing the validity and robustness of method 1 as discussed above.

Acknowledgments

Two of the authors (WL and JFV) acknowledge partial support from DIUFRO (Chile) under contract DI 07 – 0060. The third author (EEV) is grateful to FONDECYT (Chile) under contract 1060317 and Millenium Scientific Initiative under contract Millennium Science Nucleus “Basic and Applied Magnetism” P06-022-F for partial support.

References

- [1] J.W. Landry, S.N. Coppersmith, Phys. Rev. B 65 (2002) 134404.
- [2] F. Romá, F. Nieto, E.E. Vogel, A.J. Ramirez-Pastor, J. Stat. Phys. 114 (2004) 516.
- [3] J. Poulter, J.A. Blackman, J. Phys. A: Math. Gen. 34 (2001) 7527.

- [4] Bruce D. Gaulin, *Nature Materials* 4 (2005) 269.
- [5] H. Karunadasa, Q. Huang, B.G. Ueland, J.W. Lynn, P. Schiffer, K.A. Regan, R.J. Cava, *Phys. Rev. B* 71 (2005) 144414.
- [6] S.F. Edwards, P.W. Anderson, *J. Phys. F* 5 (1975) 965.
- [7] J.F. Valdés, W. Lebrecht, E.E. Vogel, *Physica A* 385 (2007) 551.
- [8] G. Toulouse, *Commun. Phys.* 2 (1977) 115.
- [9] W. Lebrecht, E.E. Vogel, J. Cartes, J.F. Valdés, *Physica A* 342 (2004) 90.
- [10] E.E. Vogel, J. Cartes, S. Contreras, W. Lebrecht, J. Villegas, *Phys. Rev. B* 49 (1994) 6018.
- [11] J.F. Valdés, J. Cartes, E.E. Vogel, S. Kobe, T. Klotz, *Physica A* 257 (1998) 557.
- [12] W. Lebrecht, J.F. Valdés, E.E. Vogel, *Physica A* 323 (2003) 466.
- [13] E.E. Vogel, W. Lebrecht, *Z. Phys. B* 102 (1997) 145.